A Predictive Control Framework for Manipulator on a Disturbed Sea-Born Platform*

Ruoyu Xu, Xiaoqiang Ji, Jiafan Hou, Hengli Liu and Huihuan Qian†

***Abstract*— In the process of landing vertical take-off and landing (VTOL) unmanned aerial vehicles (UAVs) on an unmanned surface vehicle (USV), a manipulator can be applied to help the UAV land safely and accurately. However, it is a challenge to control the manipulator on a disturbed USV due to joint velocity constraints and bandwidth limitations. To solve this problem, a predictive control framework is proposed in this paper. We leverage a first-order delay system to describe the dynamics of each joint, and control joint velocities by the model predictive controller (MPC). The time constant of the model is updated in real-time by an uncertainty observer. Simulations are conducted based on collected USV motion data to verify the proposed method, the results show that the average control accuracy is improved by 42% and 50% for position and rotation compared with the traditional inverse kinematics (IK) controller.**

I. Introduction

In the scenario of the USV-UAV cooperative landing mission, the high dynamic motion of the under-actuated USV is the primary cause of failure. The fluctuation of the landing platform can bring unexpected impact to the UAV and the ground effect can make the UAV out of control. Although there are a lot of work aim at landing a UAV on a moving platform [1], [2] or USV [3], the fluctuation of these platforms are usually slow and large landing platforms must be applied to guarantee safety. To overcome these problems, manipulator-assisted UAV landing is proposed [4], [5]. The advantage of applying the manipulator is it can assist landing by tracking and provide a balanced landing platform. Besides, external forces can be provided after a connection is established, so the UAV can land safely and accurately. What's more, the space for a large landing platform can be saved, so multiple UAVs can land on a relatively small USV. In this paper, a control framework is proposed for the floating manipulator with high dynamic base motion.

There are various methods to control the manipulator, but it is still a challenge if implemented on a disturbed sea-born platform. For the case in this paper, the manipulator needs to balance the high-frequency motion of the USV in real-time. Applying traditional control methods directly can lead to control outputs beyond the capacity of actuators, the performance can be impaired if the constraints are ignored [6]. Besides, the huge inertial of manipulator leads to lags in response. In this situation, MPC can provide the optimal solution by taking the constraints and bandwidth into consideration [7].

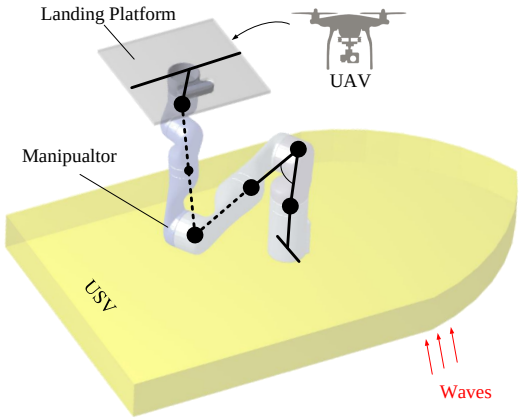

Fig. 1. An illustration of the manipulator-assisted UAV landing. The manipulator is designed to compensate the waves and track the objective to assist UAV landing.

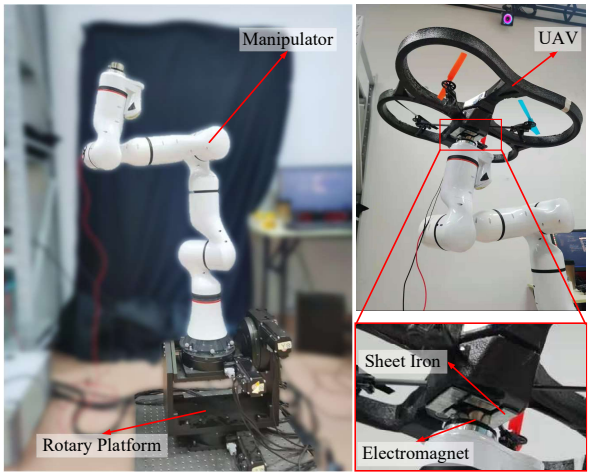

Fig. 2. Indoor experimental platform. The rotary platform can simulate the effect of waves.

II. Main Results

As shown in Fig.1, consider an n-joint serial manipulator whose base is floating with the motion of the USV. If we treat each joint of the manipulator as an independent SISO system, the closed-loop dynamic of each joint can be estimated by a first-order system in (1) [8].

$$\frac{V_i}{V_{di}} = \frac{1}{1+T_{mi}s}, \quad i = 1, ...n \tag{1}$$

*This paper is partially supported by Project U1613226 and U1813217 supported by NSFC, China, Project 2019-INT009 from the Shenzhen Institute of Artificial Intelligence and Robotics for Society, the Shenzhen Science and Technology Innovation Commission, fundamental research grant KQJSCX20180330165912672 and PF.01.000143 from The Chinese University of Hong Kong, Shenzhen.

Shenzhen Institute of Artificial Intelligence and Robotics for Society, The Chinese University of Hong Kong, Shenzhen

†Corresponding author is Huihuan Qian, email: hhqian@cuhk.edu.cn

where T_{mi} is the time constant of the joint i, V_i and V_{di} are joint velocity and desired joint velocity in s-domain. Let $\dot{\mathbf{q}}$ be the joint velocity, consider the forward kinematics of the manipulator, $\dot{\mathbf{x}} = \mathbf{J}(\mathbf{q}(\mathbf{t}))\,\dot{\mathbf{q}}$, where $\mathbf{J} \in \mathbb{R}^{6\times n}$ is the Jacobian matrix of the manipulator and $\mathbf{x} \in \mathbb{R}^6$ is the pose of the end-effector. Thereafter, we can derive (2).

$$\dot{\mathbf{x}} = \mathbf{J}(\mathbf{q}(t))\left(\dot{\mathbf{q}}_d + e^{-\mathbf{T}_m^{-1}t}(\dot{\mathbf{q}}_0 - \dot{\mathbf{q}}_d)\right) \tag{2}$$

where $\dot{\mathbf{q}}_0$ and $\dot{\mathbf{q}}_d$ is the initial and desired joint velocities in each control period, $\mathbf{T}_m = diag[T_{m1}, ..., T_{mn}]$ is the matrix related to bandwidth. $\mathbf{T}_m$ will changes with the poses of the manipulator, so we use one-step previous $\mathbf{T}_m$, $\dot{\mathbf{q}}_0$, $\dot{\mathbf{q}}_d$ and $\dot{\mathbf{q}}$ to estimate the current $\mathbf{T}_m$. This process can be realized by an uncertainty observer. According to (1), the dynamics of each joints in time domain can be expressed by (3),

$$\dot{q}_i = \dot{q}_{id} + e^{-T_{mi}^{-1}t_c}(\dot{q}_{i0} - \dot{q}_{id}), \quad i = 1, ...n \tag{3}$$

where $\dot{q}_i$ is the velocity of joint i that can be measured in each control period t_s, $\dot{q}_{id}$ is the control input. The last term of (3) is the uncertainty to be observed. Thereafter, uncertainty observer in [9] can be applied to the SISO system in (3), the observer for joint i has the form as (4).

$$\begin{cases} \hat{\dot{q}}_i = \dot{q}_d + v_0 \\ v_0 = -\lambda_0 L^{1/3}|\hat{q}_i - q_i|^{2/3}\mathrm{sgn}(\hat{q}_i - q_i) + \kappa_1 \\ \dot{\kappa}_1 = v_1 \\ v_1 = -\lambda_1 L^{1/2}|\kappa_1 - v_0|^{1/2}\mathrm{sgn}(\kappa_1 - v_0) + \kappa_2 \\ \dot{\kappa}_2 = -\lambda_2 L\mathrm{sgn}(\kappa_2 - v_1) \end{cases} \tag{4}$$

where λ_0, λ_1, λ_2 and L are parameters that can be determined by simulations, $\hat{\dot{q}}_i$, κ_1 and κ_2 are the estimation of $\dot{q}_i$, $e^{-T_{mi}^{-1}t_c}(\dot{q}_{i0} - \dot{q}_{id})$ and its derivative. Since $\dot{q}_{i0}$, which is the initial velocity of joint i, is also known in each control period, T_{mi} can be derived by the observations.

The predictive model is formulated based on a simple assumption that the Jacobian matrix is constant during the prediction horizon. Certainly, $\mathbf{J}$ will still update each control period. Then the equation (2) can be rewritten as (5) approximately in a limited time,

$$\dot{\mathbf{x}} \approx \mathbf{J}e^{-\mathbf{T}_m^{-1}t}\mathbf{J}^{-1}\dot{\mathbf{x}}_0 + \mathbf{J}(\mathbf{I} - e^{-\mathbf{T}_m^{-1}t})\dot{\mathbf{q}}_d \tag{5}$$

where $\dot{\mathbf{x}}_0$ is the initial velocity of the end-effector in Cartesian space. The pose of the end-effector can be acquired by taking the integral of (5), the result is shown in (6).

$$\begin{aligned} \mathbf{x} \approx \mathbf{x}_0 - \mathbf{J}\mathbf{T}_m\left(e^{-\mathbf{T}_m^{-1}t} - \mathbf{I}\right)\mathbf{J}^{-1}\dot{\mathbf{x}}_0 + \\ \mathbf{J}(t\mathbf{I} + \mathbf{T}_m\left(e^{-\mathbf{T}_m^{-1}t} - \mathbf{I}\right))\dot{\mathbf{q}}_d \end{aligned} \tag{6}$$

Let the control period be t_c, the state variable be $\mathbf{X}=[\mathbf{x}, \dot{\mathbf{x}}]^{\mathrm{T}}$ and the control variable be $\mathbf{u} = \dot{\mathbf{q}}_d$. The ordinary differential equations in (5) and (6) can be discretized as (7a)-(7c)

$$\mathbf{X}(k+1) = \bar{\mathbf{A}}\mathbf{X}(k) + \bar{\mathbf{B}}\mathbf{u}(k) \tag{7a}$$

$$\bar{\mathbf{A}} = \begin{bmatrix} \mathbf{I} & \mathbf{J}\mathbf{T}_m\left(\mathbf{I} - e^{-\mathbf{T}_m^{-1}t_c}\right)\mathbf{J}^{-1} \\ \mathbf{0} & \mathbf{J}e^{-\mathbf{T}_m^{-1}t_c}\mathbf{J}^{-1} \end{bmatrix} \tag{7b}$$

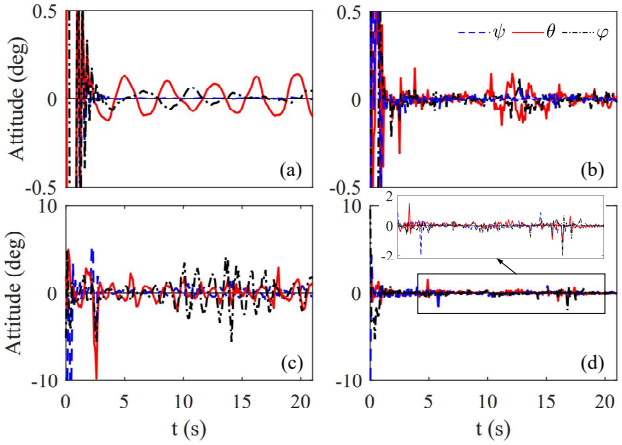

Fig. 3. The results of attitude stabilization described in C_h, the desired attitudes are marked by black lines. (a) and (b) are the simulation results of IK and MPC in the inner bay while (c) and (d) are simulated in the open sea.

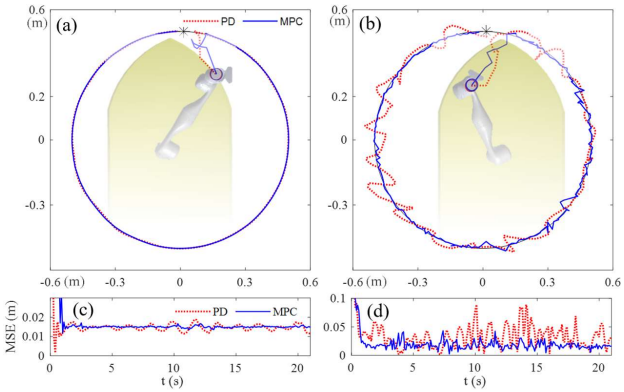

Fig. 4. The results of position control, the desired positions are marked by black lines. (a) and (b) are the simulation results in the inner bay and open sea. (c) and (d) are the tracking errors in (a) and (b).

$$\bar{\mathbf{B}} = \begin{bmatrix} \mathbf{J}\left(t_c\mathbf{I} - \mathbf{T}_m\left(\mathbf{I} - e^{-\mathbf{T}_m^{-1}t_c}\right)\right) \\ \mathbf{J}\left(\mathbf{I} - e^{-\mathbf{T}_m^{-1}t_c}\right) \end{bmatrix} \tag{7c}$$

Based on the discrete model in (7a)-(7c), the MPC problem in a control period k_t can be formulated in the form of (8a)-(8d).

$$\min_{\Delta\mathbf{u}} \quad \sum_{k=0}^{N_p}\|\mathbf{X}(k|k_t) - \mathbf{X}_d\|_{\mathbf{Q}}^2 + \sum_{j=0}^{N_c}\|\Delta\mathbf{u}(j|k_t)\|_{\mathbf{R}}^2, \tag{8a}$$

$$\text{s.t.} \quad \mathbf{X}(k|k_t) = \bar{\mathbf{A}}\mathbf{X}(k-1|k_t) + \bar{\mathbf{B}}\mathbf{u}(j-1|k_t), \tag{8b}$$

$$\mathbf{u}_{\min} \le \mathbf{u}(j|k_t) \le \mathbf{u}_{\max}, \tag{8c}$$

$$k = 1, 2, ..., N_p, \; j = 1, 2, ..., N_c, \tag{8d}$$

where (8a) is the quadratic form of the cost function, N_p is the prediction horizon, N_c is the control horizon, $\mathbf{Q}$ and $\mathbf{R}$ are penalty matrices related to errors and control increments $\Delta\mathbf{u}$, $\mathbf{X}_d$ is the reference generated by motion predictor like wavelet network [10] or auto regression. (8c) bounded the optimized control series in $[\mathbf{u}_{\min}, \mathbf{u}_{\max}]$.

III. Simulations

The proposed MPC controller is compared with the traditional inverse kinematic (IK) controller in this section.

The IK controller is implemented by Jacobian transpose method. Two groups of simulations are designed based on the USV motions collected from the inner bay and open sea, whose sea conditions are level-1 and level-3 respectively. The output of the MPC is constrained according to the joint velocity limitations, and the augment of each step is also constrained. The simulation is built based on the Robotics System Toolbox in MATLAB and KINOVA GEN3 is selected as the control objective. The state feedback is solved by the dynamic model to make the simulation more convincing. The desired attitude of the end-effector is [0 0 0], so the end-effector can be stabilized under the effect of waves. Both controllers are made to track a circular trajectory, whose radius is 0.5 m, in the dexterous workspace of the manipulator.

The results of attitudes stabilization are shown in Fig.3. According to the simulation results, the average errors of the IK controller and MPC controller in the inner bay are 0.19° and 0.11°, which are similar. And the average error of the MPC controller in the open sea is 0.52°, which is 50% lower than that of the IK controller. On the other hand, according to the trajectory tracking results in Fig.4, the average errors of IK controller and MPC controller are 1.6 cm and 1.8cm in the inner bay, and in the open sea, the average error of MPC is 2.1 cm, which is 42% lower than that of IK controller. These two controllers are similar in the low sea condition, however, the performance of the traditional control method declines significantly with the rise of the sea condition level, while the accuracy of the MPC controller is higher and changes slightly under the effect of stronger waves.

IV. Conclusion

In this paper, the end-effector stabilization problem for manipulator-assisted UAV landing on a floating marine platform is considered. To satisfy the joint constraints during the stabilizing process, a three-level MPC framework is proposed. Simulations show that the proposed control framework can improve the average control accuracy by 42% and 50% for position and rotation. The future work is the experimental implementation of the proposed method on the platform shown in Fig.2.

References

[1] T. Baca, P. Stepan, V. Spurny, D. Hert, R. Penicka, M. Saska, J. Thomas, G. Loianno, and V. Kumar, "Autonomous landing on a moving vehicle with an unmanned aerial vehicle," *Journal of Field Robotics*, vol. 36, no. 5, pp. 874–891, 2019.

[2] M. Beul, M. Nieuwenhuisen, J. Quenzel, R. A. Rosu, J. Horn, D. Pavlichenko, S. Houben, and S. Behnke, "Team nimbro at mbzirc 2017: Fast landing on a moving target and treasure hunting with a team of micro aerial vehicles," *Journal of Field Robotics*, vol. 36, no. 1, pp. 204–229, 2019.

[3] G. Shao, Y. Ma, R. Malekian, X. Yan, and Z. Li, "A novel cooperative platform design for coupled usv–uav systems," *IEEE Transactions on Industrial Informatics*, vol. 15, no. 9, pp. 4913–4922, 2019.

[4] M. Maier, A. Oeschger, and K. Kondak, "Robot-assisted landing of vtol uavs: Design and comparison of coupled and decoupling linear state-space control approaches," *IEEE Robotics and Automation Letters*, vol. 1, no. 1, pp. 114–121, 2015.

[5] M. Maier and K. Kondak, "Robot assisted landing of vtol uavs on ships: A simulation case study of the touch-down phase," in *2017 IEEE Conference on Control Technology and Applications (CCTA)*. IEEE, 2017, pp. 2094–2101.

[6] L. Dai, Y. Yu, D.-H. Zhai, T. Huang, and Y. Xia, "Robust model predictive tracking control for robot manipulators with disturbances," *IEEE Transactions on Industrial Electronics*, 2020.

[7] Y. Dai, S. Yu, Y. Yan, and X. Yu, "An ekf-based fast tube mpc scheme for moving target tracking of a redundant underwater vehicle-manipulator system," *IEEE/ASME Transactions on Mechatronics*, vol. 24, no. 6, pp. 2803–2814, 2019.

[8] A. Wahrburg and K. Listmann, "Mpc-based admittance control for robotic manipulators," in *2016 IEEE 55th Conference on Decision and Control (CDC)*. IEEE, 2016, pp. 7548–7554.

[9] Y. B. Shtessel, I. A. Shkolnikov, and A. Levant, "Smooth second-order sliding modes: Missile guidance application," *Automatica*, vol. 43, no. 8, pp. 1470–1476, 2007.

[10] S. A. Billings and H.-L. Wei, "A new class of wavelet networks for nonlinear system identification," *IEEE Transactions on neural networks*, vol. 16, no. 4, pp. 862–874, 2005.